3D Odometry based on Body Configuration

Daisuke Chugo[1], Kuniaki Kawabata[2], Hayato Kaetsu[2], Songmin Jia[1], Hajime Asama[3], Taketoshi Mishima[4]
and Kunikatsu Takase[1]

[1]Graduate School of Information Systems, The University of Electro-Communications, Tokyo, Japan
(Tel : +81-42-443-5657; E-mail: {chugo, jia, takase}@is.uec.ac.jp)
[2]Kawabata Intelligent Research Unit, Riken (The Institute of Physical and Chemical Research), Saitama, Japan
(Tel : +81-48-467-5480; E-mail: {kuniakik, kaetsu}@riken.jp)
[3]Research into Artifacts, Center for Engineering, The University of Tokyo, Chiba, Japan
(Tel : +81-4-7136-4255; E-mail: asama@race.u-tokyo.ac.jp)
[4]Faculty of Science and Engineering, Saitama University, Saitama, Japan
(Tel : +81-48-858-3497; E-mail: takemi@me.ics.saitama-u.ac.jp)

Abstract: In our current research, we are developing a holonomic mobile system which is capable of running over the step. This system realizes omni-directional motion on flat floor using special wheels and passes over non-flat ground in forward or backward direction using the passive suspension mechanism. Odometry is popular position tracking scheme for a wheeled mobile robot, however, in the case of non-flat ground, it is difficult to estimate its position using odometry because an angular relationship between wheels and ground is unknown. Therefore, in this paper, we propose a new odometry method which extends 2D odometry to the 3D space. Our key idea is using the body configuration information which changes according to the shape of the terrain. Using our idea, our mobile platform can measure the shape of terrain without external sensors. We verify the performance of our proposed control scheme by the experiments using our prototype.

Keywords: Odometry, Omni-directional wheeled vehicle, Passive linkages

1. INTRODUCTION

In recent years, mobile robot technologies are expected to perform various tasks in general structured environment such as nuclear power plants, large factories, welfare care facilities, hospitals and homes. However, there are narrow spaces with steps and slopes in such indoor environments, and it is difficult for general car-like vehicles to run around there.

Generally, the vehicle is required to have quick and efficient mobile function for effective task execution. The omni-directional mobility is useful for the tasks, especially in narrow spaces, because there is no holonomic constraint on its motion [1][2]. Furthermore, the step-overcoming function is necessary when the vehicle passes over the general environment which has vertical gaps between two or plural flat floors. Thus, in order to run around general environment, the vehicle needs to equip both of functions.

Therefore, we are developing a holonomic omni-directional vehicle with step-climbing ability [3]. Our prototype utilized new passive suspension system which is suitable for steps in the structured environment and it has seven special wheels with actuators. In order to realize the high mobility during step climbing, our vehicle drives all wheels for increasing traction force.

For practical use, it is important for the vehicle to design a reasonable mechanism that has no excessive performance. Generally, running on the structured terrain [4], the energy efficiency of the wheeled mobile system is better than the other mobile mechanisms (e.g., legged [5][6] or crawler type [7]). Thus, we adopt the universal wheel for omni-directional mobile function. The universal wheel realizes the omni-directional

mobility with the advantage of a wheeled system [8]. Furthermore, when we design a mobile robot, there are two approaches to improve the step-climbing ability of the robot. One is to improve the step-climbing ability in all the directions equally, and the other is to improve the maximum ability to pass over steps in a fixed direction with simple mechanism. If the robot has a holonomic and omni-directional mobile ability, it can change its direction in front of the step. Therefore, to realize low cost system, we design the holonomic omni-directional wheeled robot which passes the step only in forward and backward direction.

To realize the effective task execution, our vehicle is required to track its position with low cost. In general, a lot of wheeled vehicle uses an odometry for estimating its position. However, the odometry assumes that a vehicle runs on a flat floor usually and it is difficult to use the odometry for a step climbing vehicle. In previous research, many position estimating scheme are developed. Vieville [9] and Roumeliotis [10] proposed a ground shape estimating method using cameras on the vehicle and Strelow [11] proposed odometry for rough terrain using parameters of ground and wheels which are derived beforehand. However, they are requires redundant external sensors or accurate ground-wheel information, therefore, they are not suitable for practical use. On the other hand, our vehicle changes its body configuration along a terrain surface using passive linkages. This means this body configuration information reflects a ground surface.

Thus, we propose 3D odometry using body configuration information. Our proposed scheme realizes an estimation of ground surface with only internal sensors on the vehicle body.

This paper is organized as follows: we introduce the mechanical design and the controller of the vehicle in section 2; we propose novel 3D odometry scheme using body configuration information in section 3; we show the results of experiments in section 4; section 5 is conclusion of this paper.

2. MOBILE PLATFORM

2.1 Mobile Mechanism

Fig. 1 shows the prototype vehicle system. The vehicle has seven wheels and each wheel is connected to single DC motor. The size of prototype vehicle is 750[mm](L) x 540[mm](W) x 520[mm](H) and its weight is 22[kg].

The mobile mechanism consists of seven special wheels with free rollers and a passive suspension system. The special wheel equips twelve cylindrical free rollers [12] and realizes to generate the omni-directional motion using plural wheels arranged in the different direction and suitable wheel control (Fig. 2).
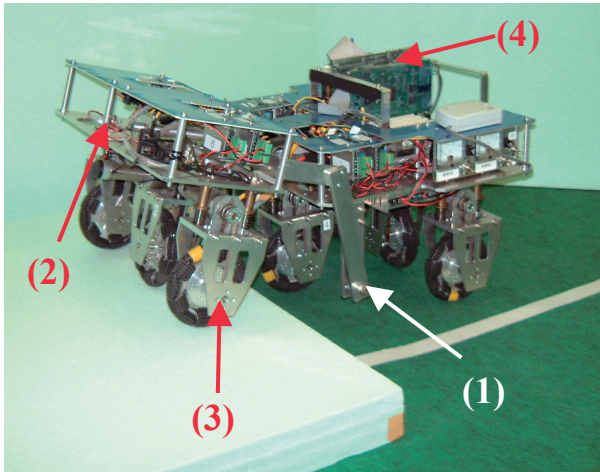
Fig. 1. Our Prototype. (1) is the passive joint 1 (pitch angle), (2) is the passive joint 2 (roll angle), (3) is the special wheel and (4) is the control computer system (CPU and I/O card).
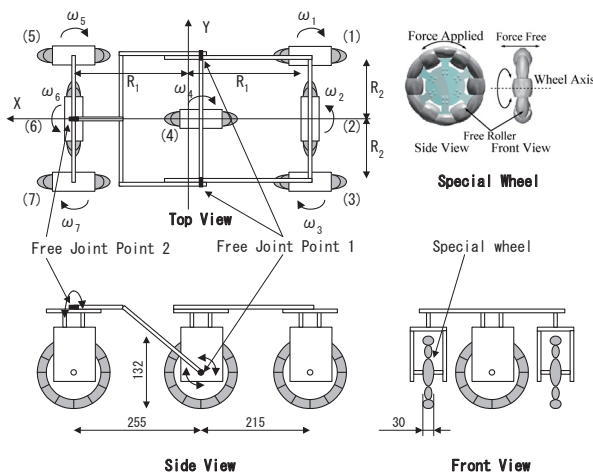
Fig. 2. Overview of the proposed mechanism.

Our mechanism utilizes new passive suspension system, which is more suitable for the step than general rocker-bogie suspensions [13] as shown in Fig. 3 [14]. The free joint point 1 is in the same height as the axle and this system helps that the vehicle can pass over the step smoothly when the wheel contacts it. (Fig. 4) No sensors and no additional actuators are equipped to pass over the irregular terrain.
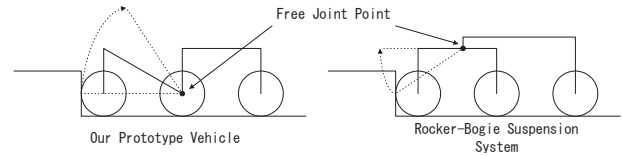
Fig. 3. New Passive Linkage Mechanism
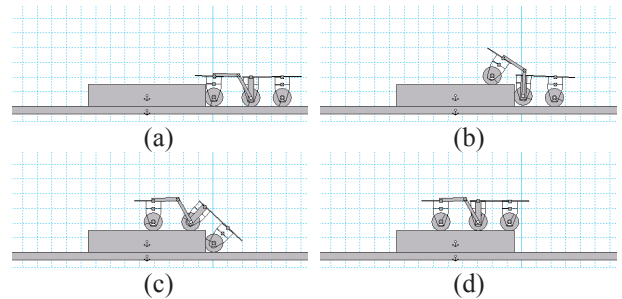
Fig. 4. Step Climbing

2.2 Controller

The control system is shown in Fig. 5. The developed vehicle has seven motor drivers, two potentiometers each joint for the configuration angle and two tilt meters for the inclination of the body. Our vehicle has redundant actuation system using seven wheels and PID-based control system [3] synchronizes the wheel rotation based on control reference, which is calculated by the kinematic model.
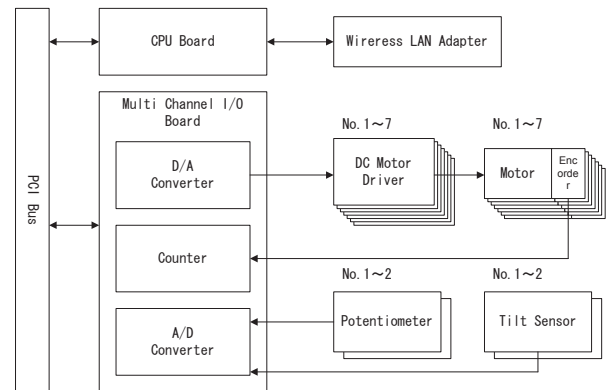
Fig. 5. Overview of the vehicle's control system

3. 3D ODOMETRY

3.1 Kinematics of Passive Linkages

Our vehicle has the passive linkage mechanism in its body and the body configuration changes according to the terrain condition when the vehicle passes over the step as shown in Fig. 4. Therefore, it is required to modify the traveling direction vector of wheel referring

to its configuration for odometry with step climbing.

In this paragraph, we consider the relationship of rotation velocity vector of each wheel and the change of the body configuration on general passive linkage vehicle model.

We assume that the vehicle has n passive linkages and all wheels have grounded and actuated. When the vehicle passes over the barrier as shown in Fig. 6, the velocity vector of wheel $i+1$ is calculated by the velocity vector of wheel i and the rotation velocity vector of wheel i+1 in (1). These vectors are expressed by three dimensions in their local coordination system.

$$ {}^i\mathbf{v}_{i+1} = {}^i\mathbf{v}_i + {}^i\boldsymbol{\sigma}_i \times {}^i\mathbf{P}_{i+1}^i \tag{1} $$

where i is the number of wheel ($i = 1 \cdots n$), ${}^i\mathbf{v}_i$ and ${}^i\mathbf{v}_{i+1}$ are the velocity vectors of wheel i and $i+1$ on the coordination{i}, respectively. ${}^i\boldsymbol{\sigma}_i$ is the rotation vector of linkage i on the coordination{i}. ${}^i\mathbf{P}_{i+1}^i$ is the position vector from the wheel i to wheel $i+1$.
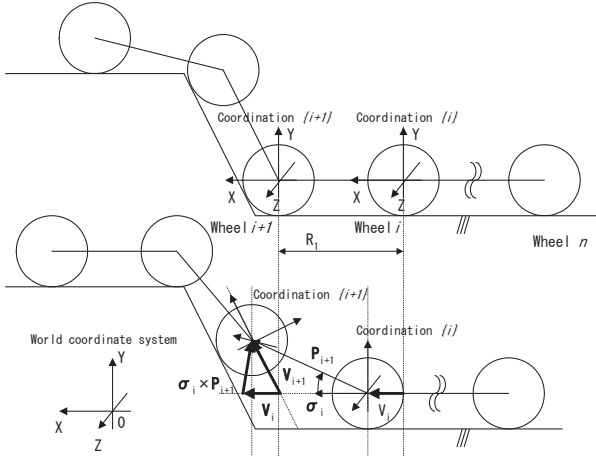
Fig. 6. Passive linage model.

3.2 Adaptation for Odometry of Wheel

The velocity vector of the wheel has the following features.

- Its direction is the same as the driving direction of the wheel.
- Its direction is the same as the perpendicular direction to the terrain surface which the wheel is grounded on.

In consideration of the previous conditions, we define the coordination of each wheel as shown in Fig. 7.
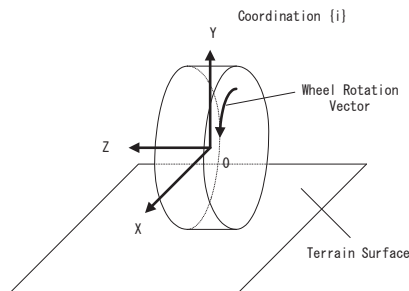
Fig. 7. The definition of the coordination of the wheel

- The x-axis is defined in the drive direction of the wheel.
- The y-axis is defined in the perpendicular direction to the ground.

The traveling distance of wheel is derived by the velocity of the driving-direction ingredient and the rotation of the linkage which the wheel is connected on. Therefore, using this definition, the x-direction ingredient of the velocity vector and the rotation vector focusing on z-axis in the coordination {i} derive the traveling distance. The traveling distance value of the wheel i+1 (ω_{i+1}) is derived from (2) and (3).

$$ \omega_{i+1} = \frac{\left\| {}^{i+1}\mathbf{v}_{i+1} \right\|_x}{r_{i+1}} + \left\| {}^i\boldsymbol{\sigma}_i \right\|_z \tag{2} $$

$$ {}^{i+1}\mathbf{v}_{i+1} = {}^{i+1}_i\mathbf{R} \cdot {}^i\mathbf{v}_{i+1} \tag{3} $$

$\left\| {}^{i+1}\mathbf{v}_{i+1} \right\|_x$ is x ingredient of the wheel $i+1$ velocity vector, $\left\| {}^i\boldsymbol{\sigma}_i \right\|_z$ is the ingredient of rotation vector focusing on z-axis, r_{i+1} is the radius of the wheel $i+1$ and ${}^{i+1}_i\mathbf{R}$ is the conversion matrix from the coordination {i} to the coordination {i+1}. Thus, when the velocity vector and rotation vector of wheel i are defined as ${}^i\mathbf{v}_i$ and ${}^i\boldsymbol{\sigma}_i$, the traveling distance of wheel $i+1$ is expressed as (4).

$$ \omega_{i+1} = \frac{\left\| {}^{i+1}_i\mathbf{R} \cdot \left({}^i\mathbf{v}_i + {}^i\boldsymbol{\sigma}_i \times {}^i\mathbf{P}_{i+1}^i \right) \right\|_x}{r_i} + \left\| {}^i\boldsymbol{\sigma}_i \right\|_z \tag{4} $$

The passive body linkage mechanism is designed that all wheels have grounded, therefore we can assume that each wheel grounds the plane. When the angle between the x-axis of coordination {i} and the one of coordination {i+1} is α_i, the conversion matrix is derived as (5). α_i is fulfill (6), because the wheel does not float from the ground.

$$ {}^{i+1}_i\mathbf{R} = \begin{bmatrix} \cos\alpha_i & -\sin\alpha_i & 0 \\ \sin\alpha_i & \cos\alpha_i & 0 \\ 0 & 0 & 1 \end{bmatrix} \tag{5} $$

$$ \left\| {}^{i+1}\mathbf{v}_{i+1} \right\|_y = 0 \tag{6} $$

$\left\| {}^{i+1}\mathbf{v}_{i+1} \right\|_y$ is y ingredient of the wheel $i+1$ velocity vector.

3.3 Adaptation to Our Prototype

In previous paragraph, we discuss the vehicle kinematics and traveling distance of wheels referring to the body configuration. In this paragraph, we adapt the proposed derivation scheme to our prototype vehicle.

Our vehicle measures the change of body configuration using its attitude sensors and derives the traveling distance of wheels with this information.

Our prototype vehicle is two-linkage model as shown in Fig. 8. The vehicle has two free joints and each joint has potentiometers and tilt sensors are attached on the rear part of the vehicle body. We can measure the following angles using these sensors.

- The roll angle θ_1 and pitch angle γ_1 of the body shape from potentiometers.
- The roll angle θ_2 and pitch angle γ_2 of the body inclination from tilt sensors.
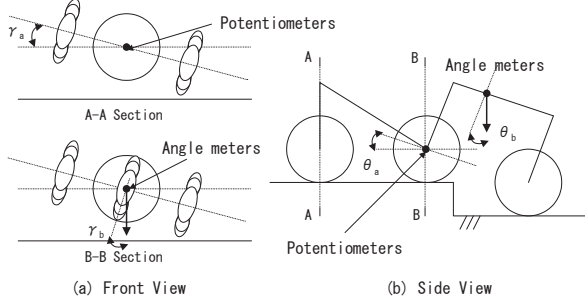
Fig. 8. The angle meters.

Our developing vehicle has 7 wheels and all wheels has actuated. Fig. 2 shows the definition of the wheel number (We display as wheel i: $i = 1 \cdots 7$), the coordinates, the length of each links, and the rotate speed of each wheel, respectively. R_1 and R_2 indicate the length of each links and $\omega_1, \cdots, \omega_7$ are the rotation velocity of each wheel. Fig. 9 shows the positional relationship between wheels and angles. Our vehicle passes over the obstacles in forward or backward direction, therefore, we discuss wheel 1,3,4,5 and 7.

When the vehicle runs at v_0 in x-direction on the coordination {4}, the velocity vector of wheel 7 on the coordination {4} is derived as (7) by (1).

$$
\begin{aligned}
{}^4\mathbf{v}_7 &= {}^4\mathbf{v}_6 + {}^4\boldsymbol{\omega}_6 \times {}^4\mathbf{P}_7^6 \\
&= \left({}^4\mathbf{v}_4 + {}^4\boldsymbol{\omega}_4 \times {}^4\mathbf{P}_6^4 \right) + {}^4\boldsymbol{\omega}_6 \times {}^4\mathbf{P}_7^6 \\
&= \begin{bmatrix} {}^4v_{7x} & {}^4v_{7y} & {}^4v_{7z} \end{bmatrix}^T
\end{aligned} \tag{7}
$$

$$
= \begin{bmatrix} v_0 + \dot{\theta}_1 \{ -R_1 \sin\theta_1 + R_2 \cos\theta_1 \sin\gamma_1 - b\cos\theta_1 (1 - \cos\gamma_1) \} \\ \dot{\theta}_1 \left\{ \begin{array}{l} R_1 \cos\theta_1 - R_2 \sin\theta_1 \sin\gamma_1 \\ + b\sin\theta_1 (1 - \cos\gamma_1) \end{array} \right\} - \dot{\gamma}_1 (R_2 \cos\gamma_1 - b\sin\gamma_1) \\ -\dot{\gamma}_1 (R_2 \cos\theta_1 \sin\gamma_1 - b\cos\theta_1 (1 - \cos\gamma_1)) \end{bmatrix}
$$

As the same, the velocities of wheel 1, 3 and 5 are derived.

$$
{}^4\mathbf{v}_1 = \begin{bmatrix} {}^4v_{1x} & {}^4v_{1y} & {}^4v_{1z} \end{bmatrix}^T \tag{8}
$$

$$
= \begin{bmatrix} v_0 - \dot{\theta}_2 \{ R_1 \sin\theta_2 + R_2 \cos\theta_2 \sin\gamma_2 - b\cos\theta_2 (1 - \cos\gamma_2) \} \\ \dot{\theta}_2 \left\{ \begin{array}{l} R_1 \cos\theta_2 + R_2 \sin\theta_2 \sin\gamma_2 \\ - b\sin\theta_2 (1 - \cos\gamma_2) \end{array} \right\} + \dot{\gamma}_2 (R_2 \cos\gamma_2 - b\sin\gamma_2) \\ \dot{\gamma}_2 (R_2 \cos\theta_2 \sin\gamma_2 - b\cos\theta_2 (1 - \cos\gamma_2)) \end{bmatrix}
$$
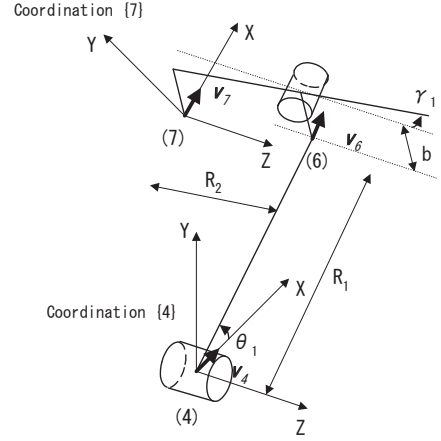
Fig. 9. Coordination and Parameters.

$$
{}^4\mathbf{v}_3 = \begin{bmatrix} {}^4v_{3x} & {}^4v_{3y} & {}^4v_{3z} \end{bmatrix}^T \tag{9}
$$

$$
= \begin{bmatrix} v_0 + \dot{\theta}_2 \{ -R_1 \sin\theta_2 + R_2 \cos\theta_2 \sin\gamma_2 - b\cos\theta_2 (1 - \cos\gamma_2) \} \\ \dot{\theta}_2 \left\{ \begin{array}{l} R_1 \cos\theta_2 - R_2 \sin\theta_2 \sin\gamma_2 \\ + b\sin\theta_2 (1 - \cos\gamma_2) \end{array} \right\} - \dot{\gamma}_2 (R_2 \cos\gamma_2 - b\sin\gamma_2) \\ -\dot{\gamma}_2 (R_2 \cos\theta_2 \sin\gamma_2 - b\cos\theta_2 (1 - \cos\gamma_2)) \end{bmatrix}
$$

$$
{}^4\mathbf{v}_5 = \begin{bmatrix} {}^4v_{5x} & {}^4v_{5y} & {}^4v_{5z} \end{bmatrix}^T \tag{10}
$$

$$
= \begin{bmatrix} v_0 - \dot{\theta}_1 \{ R_1 \sin\theta_1 + R_2 \cos\theta_1 \sin\gamma_1 - b\cos\theta_1 (1 - \cos\gamma_1) \} \\ \dot{\theta}_1 \left\{ \begin{array}{l} R_1 \cos\theta_1 + R_2 \sin\theta_1 \sin\gamma_1 \\ - b\sin\theta_1 (1 - \cos\gamma_1) \end{array} \right\} + \dot{\gamma}_1 (R_2 \cos\gamma_1 - b\sin\gamma_1) \\ \dot{\gamma}_1 (R_2 \cos\theta_1 \sin\gamma_1 - b\cos\theta_1 (1 - \cos\gamma_1)) \end{bmatrix}
$$

The rotation vector of each body linkage is derived using the roll and pitch angle as shown in (11) and (12). The linkage 5 and linkage 7 is the same rigid body, therefore ${}^4\boldsymbol{\sigma}_5$ and ${}^4\boldsymbol{\sigma}_7$ is same. The same relationship is realized also about ${}^4\boldsymbol{\sigma}_1$ and ${}^4\boldsymbol{\sigma}_3$.

$$
{}^4\boldsymbol{\sigma}_5 = {}^4\boldsymbol{\sigma}_7 = \begin{bmatrix} {}^4\sigma_{7x} & {}^4\sigma_{7y} & {}^4\sigma_{7z} \end{bmatrix}^T = \begin{bmatrix} \dot{\gamma}_1 & 0 & \dot{\theta}_1 \end{bmatrix}^T \tag{11}
$$

$$
{}^4\boldsymbol{\sigma}_1 = {}^4\boldsymbol{\sigma}_3 = \begin{bmatrix} {}^4\sigma_{3x} & {}^4\sigma_{3y} & {}^4\sigma_{3z} \end{bmatrix}^T = \begin{bmatrix} \dot{\gamma}_2 & 0 & \dot{\theta}_2 \end{bmatrix}^T \tag{12}
$$

As shown in (5), we assume that the obstacle is the α_i degree slope about wheel i. The velocity vector and the traveling distance of wheel i are expressed in (13) and (14). The α_i degree is defined in (15), because the x-axis is defined in the drive direction of the wheel and the velocity vector is parallel to the drive direction as (6). Using these equations, traveling distance of all wheel are derived based on wheel 4.

$$
{}^i\mathbf{v}_i = {}^i_4\mathbf{R} \cdot {}^4\mathbf{v}_i = \begin{bmatrix} \cos\alpha_i & -\sin\alpha_i & 0 \\ \sin\alpha_i & \cos\alpha_i & 0 \\ 0 & 0 & 1 \end{bmatrix} \cdot \begin{bmatrix} {}^4v_{ix} \\ {}^4v_{iy} \\ {}^4v_{iz} \end{bmatrix} \tag{13}
$$

$$
= \begin{bmatrix} \cos\alpha_i \cdot {}^4v_{ix} - \sin\alpha_i \cdot {}^4v_{iy} \\ \sin\alpha_i \cdot {}^4v_{ix} + \cos\alpha_i \cdot {}^4v_{iy} \\ {}^4v_{iz} \end{bmatrix}
$$

$$\omega_i = \frac{\cos\alpha_i \cdot {}^4v_{ix} - \sin\alpha_i \cdot {}^4v_{iy}}{r} + {}^4\sigma_z^i \qquad (14)$$

$$\sin\alpha_i \cdot {}^4v_{ix} + \cos\alpha_i \cdot {}^4v_{iy} = 0 \qquad (15)$$

Our vehicle uses the traveling distance of wheel 7 based on wheel 4 in forward direction and the traveling distance of wheel 3 in backward direction for 3D odometry, because our vehicle can pass over the obstacle only in forward and backward direction.

3.4 Coordination of Wheel Rotation Velocity

In previous paragraph, we discuss traveling distance of wheels referring to the body configuration on our prototype. This means that even if the vehicle passes over the obstacle with constant speed, the wheel should change its rotation velocity according to its body configuration. The unsuitable rotation velocity of wheel, which is calculated by fixed kinematics model, will cause to make the wheel slippage, and the accuracy of odometry will become poor.

In general, mobile vehicle for rough terrain uses traction control scheme for wheel control. In our previous works, we discussed the wheel feedback control system considering with the output traction of each wheel [3]. However, it is difficult to coordinate the rotation velocities of each wheel using only the traction control, especially, when the change of body configuration is large.

Therefore, in our vehicle system, we coordinate the wheel control reference according to the kinematics model in previous paragraphs using (7)-(14) [15].

4. EXPERIMENT

4.1 Experimental Setup

We verify the performance of our odometry scheme by the experiment using our prototype. Table 1 shows the vehicle parameters. In this experiment, the prototype vehicle passes over the step from forward direction as Fig. 10 and we verify on two cases.

In first case, the vehicle passes over a wood step. Its height is 30[mm] and its length is 500[mm]. In second case, the vehicle passes over a styrene foam step. Its height is 60[mm] and its length is 500[mm]. In both cases, the vehicle velocity is 0.25[m/sec] and utilized our PID based controller which coordinates the rotation velocity reference of each wheel according to the body configuration [15].
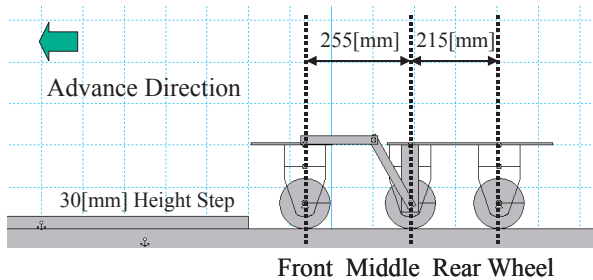
Fig. 10. Experimental Setup.

In order to verify that proposed system is effective, we compare the result by our proposed system with the result utilizing standard system, which uses only the traveling distance of wheel 4 and angle meters. This odometry scheme is standard for normal wheeled vehicle and it does not consider the body shape. Furthermore, fixed wheel control reference is utilized which does not consider its body configuration.

Table 1. The Vehicle Parameters

Length	Front 195[mm],Rear 400[mm]
Body Weight	Front 7.8[kg], Rear 13.8[kg], Link 0.6[Kg]
Wheel diameter	132[mm]
Distance between wheels	Front 255[mm], Rear 215[mm]
Center of Gravity	Front: on the front wheel
	Rear: 105[mm] from middle to rear wheel
Friction coefficient	Static 0.4, Dynamic 0.3
Running speed	0.25[m/sec]

4.2 Experimental Results

Fig.11 and Fig.12 show a motion of our prototype vehicle and Fig.13 and Fig.14 show the odometry results. From Fig.13 and Fig.14, our vehicle can estimate the shape of a step. The edge of the step rounds in the estimated shape because of wheels.

Fig.15 shows the slippage ratio of middle wheel. (i=4) The slip ratio [16] are calculated by (16). From results of Fig.16, we can verify that our wheel velocity coordination system reduces wheel slippage.

$$\hat{s}_i = \frac{r_i\omega_i - v_i}{r_i\omega_i} \qquad (16)$$

ω_i is the rotation speed of the wheel. r_i and v_i indicate the radius of the wheel and the vehicle speed, respectively.

Using our proposed odometry scheme, the estimation error reduces 58[%] in case 1 and 72[%] in case 2. The estimation error in case 2 is larger than one in case 1, because in case 2, vertical gap is larger than case 1 and there is more wheel slippage as shown in Fig.16. However, in both cases, using our proposed scheme, the wheel slippage reduces and the odometry accuracy improves.

Therefore, our 3D odometry scheme is effective for the wheeled vehicle with passive linkages.

(a)   (b)

Fig.11   Passing over 30[mm] height step.
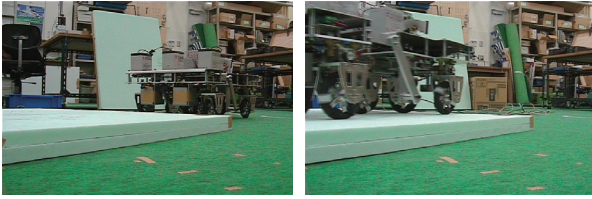
Fig.12   Passing over 60[mm] height step.
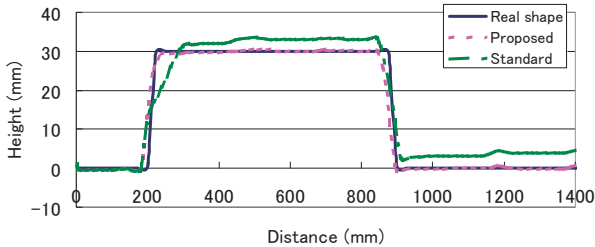
Fig.13. Odometry Result of 30[mm] height step.
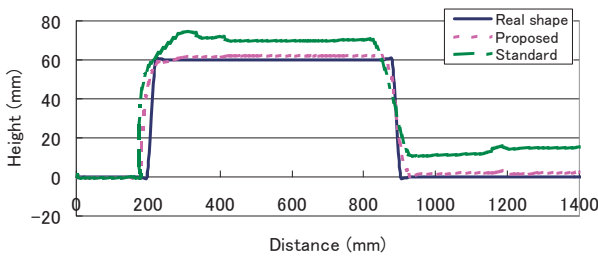
Fig.14. Odometry Result of 60[mm] height step.
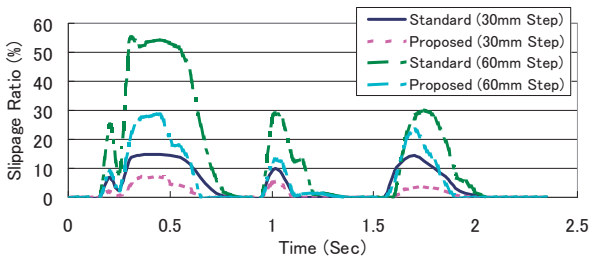
Fig.15. Slippage ratio during step climbing.

5. CONCLUTION

In this paper, we propose new odometry scheme for rough terrain using the body configuration information. Our scheme realizes 3D odometry with only internal sensor on the vehicle body.

We verified the effectiveness of our proposed scheme by the experiments using our prototype. Utilizing our proposed scheme, the slip ratio of the wheel reduces and odometry accuracy is improved.

In our future work, we discuss the wheel control scheme for reducing slippage during step climbing.

REFERENCES

[1]   G. Campion, G. Bastin and B.D. Andrea-Novel, "Structual Properties and Classification of Kinematic and Dynamic Models of Wheeled Mobile Robots," *IEEE Trans. on Robotics and Automation*, Vol.12, No.1, pp.47-62, 1996.

[2]   M. Ichikawa, "Wheel arrangements for Wheeled Vehicle," *J. of the Robotics Society of Japan*, Vol.13, No.1, pp.107-112, 1995.

[3]   D. Chugo, K. Kawabata, H. Kaetsu, H. Asama, T. Mishima, "Development of Omni-Directional Vehicle With Step-Climbing Ability", *Proc. of the 2003 IEEE Int. Conf. on Robotics and Automation*, pp.3849-3854, 2003.

[4]   M. Thianwiboon, V. Sangveraphunsiri and R. Chancharoen, "Rocker-Bogie Suspension Performance," *Proc. of the 11th Int. Pacific Conf. in Automotive Engineering*, IPC2001D079, 2001.

[5]   G. Endo and S. Hirose, "Study on Roller-Walker: System Integration and Basic Experiments", *Proc of the 1999 IEEE Int. Conf. on Robotics and Automation*, pp.2032-2037, 1999.

[6]   H. Hirukawa, S. Kajita, F. Kanehiro, K. Kaneko and T. Isozumi, "The Human-Size Humanoid Robot That Can Walk, Lie Down and Get Up," *Int. J. of Robotics Research*, Vol.24, No.9, pp.755-769, 2005.

[7]   S. Hirose and S. Amano, "The VUTON: High Payload, High Efficiency Holonomic Omni-Directional Vehicle", *Proc. of the 6th Symp. on Robotics Research*, pp.253-260, 1993.

[8]   L. D. Ferriere and G. Campion, "Design of Omnimobile Robot Wheels", *Proc. of the 1996 IEEE Int. Conf. on Robotics and Automation*, pp.3664-3670, 1996.

[9]   T. Vieville, F. Romann, B. Hotz, H. Mathieu, M. Buffa, L. Robert, P.E.D.S. Facao, O.D. Faugeras and J.T. Audren, "Autonomous navigation of a mobile robot using inertial and visual cues," *Proc. of the 1993 IEEE/RSJ Int. Conf. on Intelligent Robots and Systems*, pp.360-367, 1993.

[10]   S.I. Roumeliotis, A.E. Johnson and J.F. Montgomery, "Augmenting inertial navigation with image-based motion estimation," *Proc. of the 2002 IEEE Int. Conf. on Robotics and Automation*, pp.4326-4333, 2002.

[11]   D. Strelow, J. Mishler, S. Singh and H Herman, "Extending shape from motion to noncentral omnidirectional cameras," *Proc. of the 2001 IEEE/RSJ Int. Conf. on Intelligent Robots and Systems*, pp.2086-2092, 2001.

[12]   H. Asama, M. Sato, L. Bogoni, H. Kaetsu, A. Matsumoto and I. Endo, "Development of an Omni-Directional Mobile Robot with 3 DOF Decoupling Drive Mechanism", *Proc. of the 1995 IEEE Int. Conf. on Robotics and Automation*, pp.1925-1930, 1995.

[13]   H. W. Stone, "Mars Pathfinder Microrover: A Low-Cost, Low-Power Spacecraft", *Proc. of the 1996 AIAA Forum on Advanced Developments in Space Robotics*.

[14]   D. Chugo, K. Kawabata, H. Kaetsu, H. Asama and T. Mishima, "Mechanical Design of Step-Climbing Vehicle with Passive Linkages," *Bioinspiration and Robotics: Climbing and Walking Robots*, pp.429-440, 2007. (ISBN 978-3-902613-15-8)

[15]   D. Chugo, K. Kawabata, H. Kaetsu, H. Asama and T. Mishima, "Omni-directional Vehicle Control Based on Body Configuration," *Industrial Robot*, Vol.35, No.3, 2008. (in press)

[16]   K. Yoshida, and H. Hamano, "Motion Dynamic of a Rover With Slip-Based Traction Model", *Proc. of the 2002 IEEE Int. Conf on Robotics and Automation*, pp.3155-3160, 2002.